Far-Infrared N/O Abundance Estimates for Dusty Galaxies

Bo Peng
Cornell

Cody Lamarche (University of Toledo)
Gordon Stacey
Thomas Nikola
Christopher Rooney
Carl Ferkinhoff (WSU)
Amit Vishwas
Catie Ball
Drew Brisbin (JAO)
James Higdon (GSU)
Sarah Higdon (GSU)

SOFIA Tele-talk
7 April 2021

Arp 299 credit: NRAO/VLA, HST

Content

- Background
- Far-IR N/O diagnostics
- Photoionisation model grids calibration with Neon lines
- SOFIA FIFI-LS data
- Application on nearby galaxies
- Summary and prospects

The Astrophysical Journal, 908:166 (14pp), 2021 February 20 https://doi.org/10.3847/1538-4357/abd4e2

Far-Infrared Line Diagnostics: Improving N/O Abundance Estimates for Dusty Galaxies

B. Peng[1], C. Lamarche[2], G. J. Stacey[1], T. Nikola[3], A. Vishwas[3], C. Ferkinhoff[4], C. Rooney[1], C. Ball[1], D. Brisbin[5], J. Higdon[6], and S. J. U. Higdon[6]
[1] Department of Astronomy, Cornell University, Ithaca, NY 14853, USA; bp392@cornell.edu
[2] Department of Physics and Astronomy, University of Toledo, 2801 West Bancroft Street, Toledo, OH 43606, USA
[3] Cornell Center for Astrophysics and Planetary Science, Cornell University, Ithaca, NY 14853, USA
[4] Department of Physics, Winona State University, Winona, MN 55987, USA
[5] Joint ALMA Observatory, Alonso de Cordova 3107, Vitacura, Santiago, Chile
[6] Department of Physics, Georgia Southern University, Statesboro, GA 30460, USA
Received 2020 September 4; revised 2020 December 15; accepted 2020 December 16; published 2021 February 22

N/O: Nitrogen-to-Oxygen abundance ratio

Intermediate mass stars
primary + secondary

Massive stars
primary

- **Age, star formation history**
- **N/O - O/H relation**

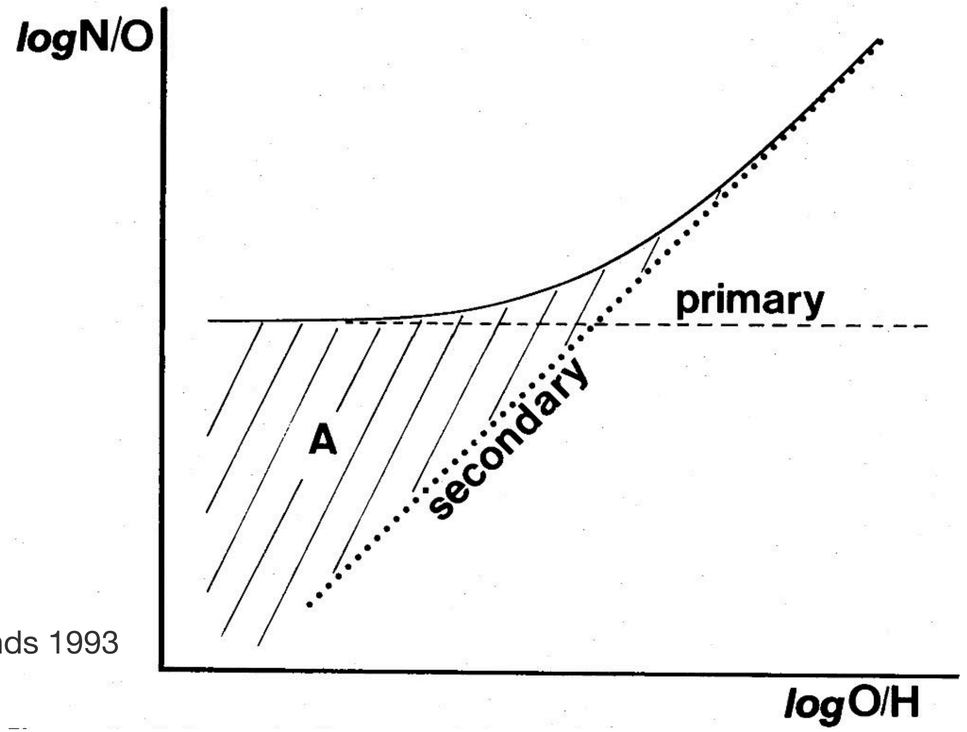

Vila-Costas & Edmunds 1993

Background: N/O - O/H relation

- N/O - O/H relation well established
- No evolution up to z ~ 0.4
- Affected by SFE, SF pattern (continuous or busty), feedback …

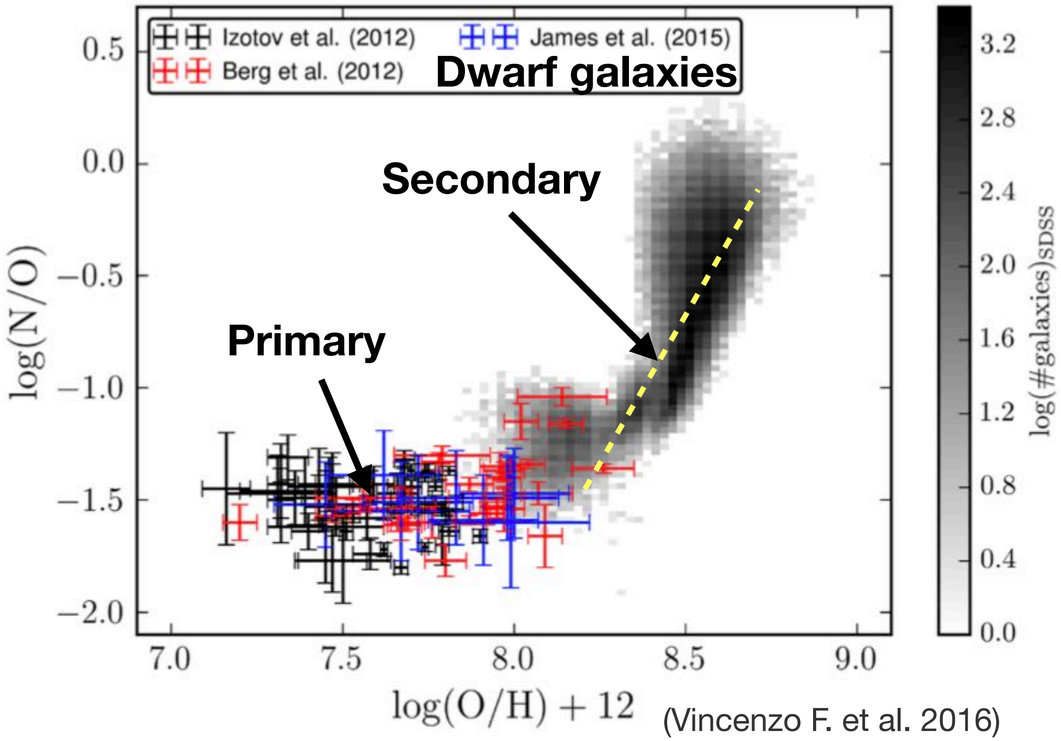

(Vincenzo F. et al. 2016)

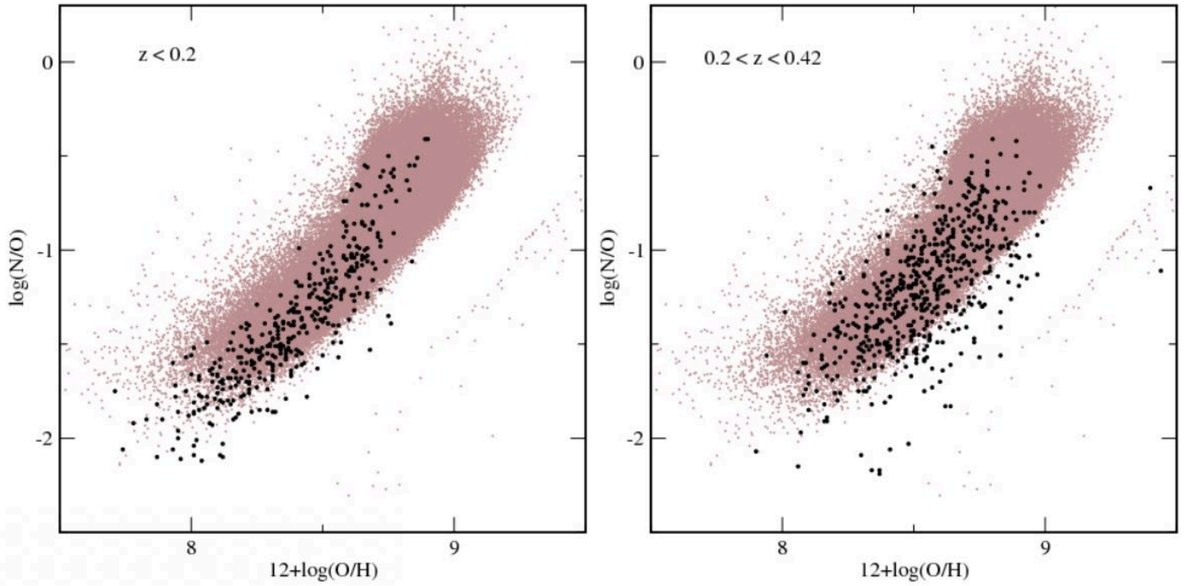

Perez-Montero et al. 2013

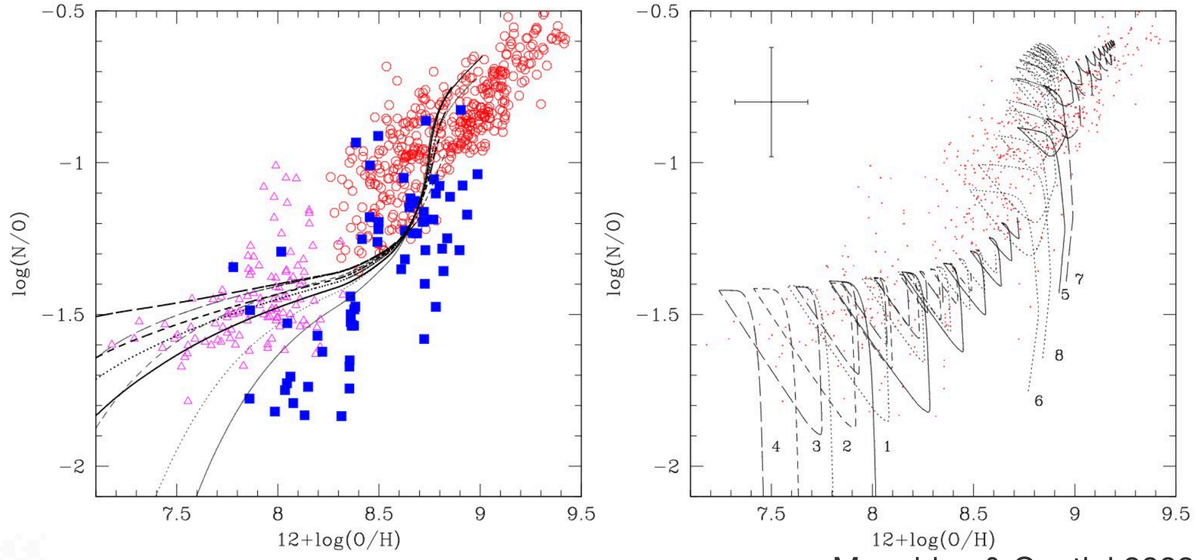

Mouchine & Contini 2002

Implicit appearance in

- **Metallicity diagnostics**

  [N II]/Hα, [N II]λ6584/[O II]λ3727, [N II]λ6584/[O III]λ5007,

  [O III]52+88/[N III], [O III]88/[N II]122, etc.

- **Photoionisation models**

  input parameter of abundance

- **BPT diagram**

  [N II]/Hα to [O III]/Hβ

N/O-O/H relation

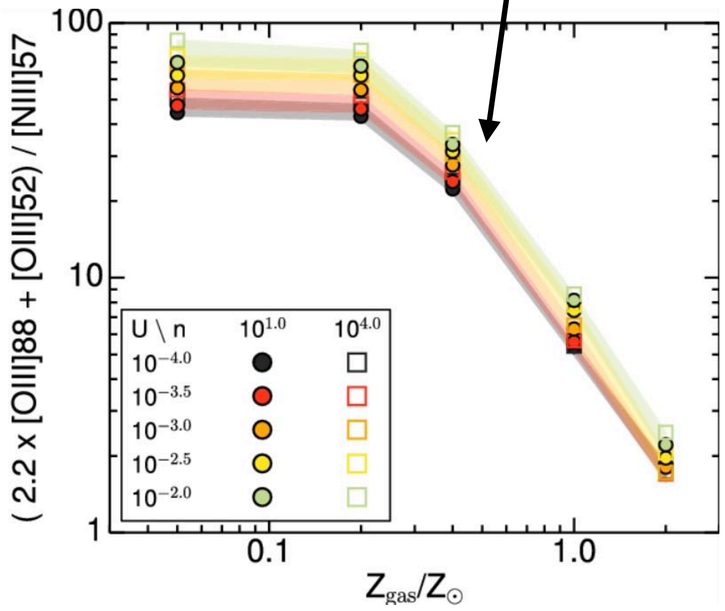

Pereira-Santaella et al. 2017

N/O diagnostics

- **Optical strong line method**

  N2O2 ([N II]λ6584/[O II]λ3727), N2S2 ([N II]λ6584/[S II]),

  N2R2 ([N II]λ6584/Hβ + [O II]λ3727/Hβ)

- **Te methods**

- **Far-IR strong line**

  [N III] 57 μm/[O III] 52 μm. Only on H II regions and PNs.

Far-IR Fine-structure lines

- Insensitive to electron temperature
- Moderate dependence on density
- Little-to-none dust extinction
- Atmosphere absorption, low transmission
- Strong

Clear physical interpretation

Difficult to detect

Density weighted

Optical forbidden lines

- Exponential dependence on temperature
- Moderate dependence on density
- Require extinction correction
- Good observation condition
- Strong

Difficult to interpret

Easy to detect

Temperature weighted

Line ratio

$$\frac{Flux(X^{a+}_{i\rightarrow j})}{Flux(Y^{b+}_{k\rightarrow l})} = \frac{X}{Y} \cdot \frac{X^{a+}/X}{Y^{b+}/Y} \cdot \frac{X^{a+}_{i}/X^{a+}}{Y^{b+}_{k}/Y^{b+}} \cdot \frac{A_{i\rightarrow j}E_{i\rightarrow j}}{A_{k\rightarrow l}E_{k\rightarrow l}}$$

Abundance

Ionisation fraction

(radiation field strength/hardness)

Energy level distribution

(density, temperature)

Transition probability and energy

[N III] 57 μm/[O III] 52 μm

Ionisation fraction

Ion	O II	N II	He II	N III	O III
Ionization energy (eV)	13.62	14.53	24.59	29.60	35.12

Highly ionised, only exist in H II region

no contamination from DIG and neutral gas

Co-spatial in He Strömgren sphere

$\frac{N^{2+}/N}{O^{2+}/O} \sim 1$ in hard radiation field, weakly dependent on hardness

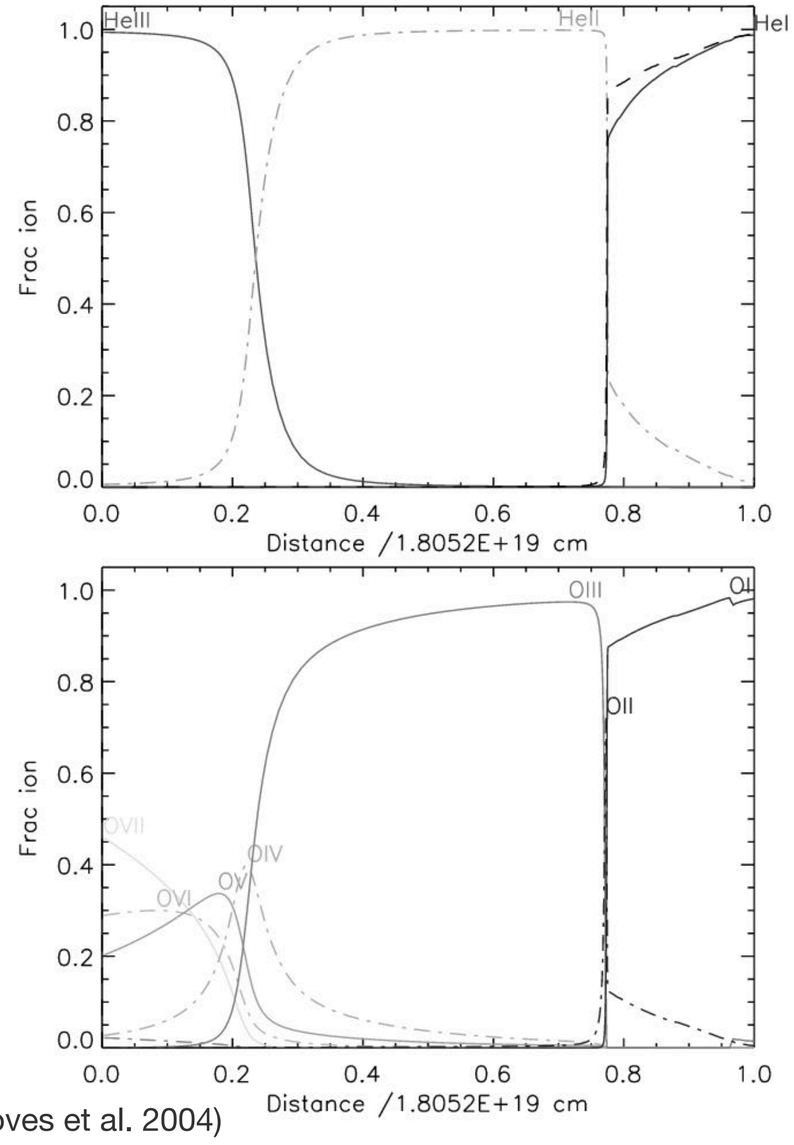

(Groves et al. 2004)

Energy level distribution

Ion	Line wavelength (μm)	Critical density (cm^-3)
N III	57.32	2.1E+03
O III	51.81	3.6E+03
	88.36	510

Close in critical density

$$\frac{\epsilon_{[\mathrm{N\ III}]}}{\epsilon_{[\mathrm{O\ III}]52}}$$

function of electron density, change by 5 from low to high density limit, can be corrected

Other benefits

- proximity in wavelength
- [O III]52 bright
- [O III]52/88 probing n_e in the same region

N3O3 parameter

emissivity ratio at low density limit

$$N/O \sim N3O3 = \frac{F_{[\mathrm{N\ III}]}}{F_{[\mathrm{O\ III}]52}} \times 0.400$$

With density correction

$$N/O \sim N3O3_{n_e} = N3O3 \times \frac{1 + 0.691 n_e/T_e^{1/2} + 0.0966 n_e^2/T_e}{1 + 0.377 n_e/T_e^{1/2} + 0.0205 n_e^2/T_e}$$

$$= N3O3 \times 6.82 \frac{R_{52/88}\left(R_{52/88} + 1.01\right)}{2.13 + 6.26 R_{52/88} + R_{52/88}^2}$$

Replace density factor by [O III]52/88 line ratio

3MDB: A virtual observatory for photoionized nebulae (Morisset et al. 2015)

- Data repository of photoionisation grids
- Cloudy
- Stellar population synthesis
- **Independent N/O input**

- **BOND** n_e **= 100 cm^-3**

  Vale Asari et al. 2016

- **CALIFA** n_e **= 10 cm^-3**

  Cid Fernandes et al. 2014

Match in parameter space

- log U = -4 to -1.5, Δ log U = 0.5
- Age = 1, 3, 4, 6 Myr
- log O/H = -3.2, to -4.0, Δ log O/H = 0.2
- log N/H = -1.25 to -0.25, Δ log N/H = 0.25

→ 480 + 480 = 960 models

Radiation hardness indicator

- [N III]/[N II]
- [Ne III]15.6/[Ne II]12.8 can probe very hard radiation field; strongly correlated with N++/O++ ionisation fraction

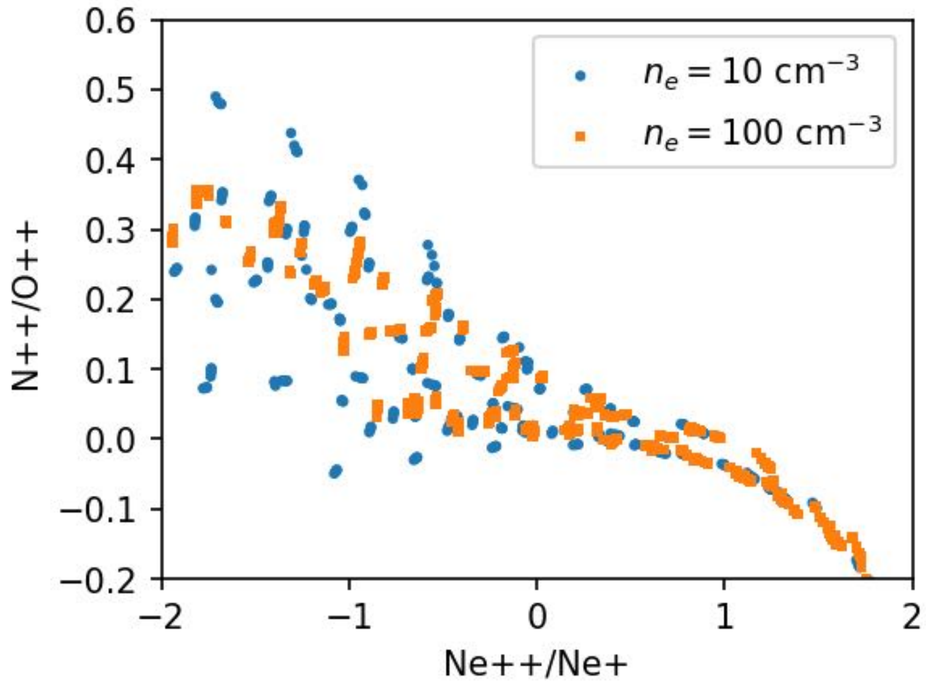

Ion	N II	Ne II	He II	N III	Ne III
Ionisation energy (eV)	14.53	21.56	24.59	29.60	40.96

Calibration

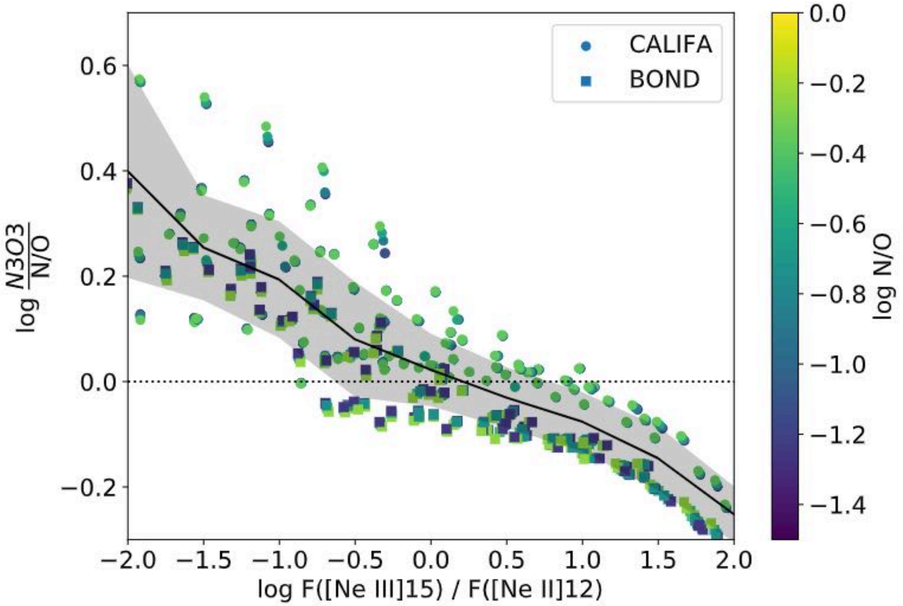

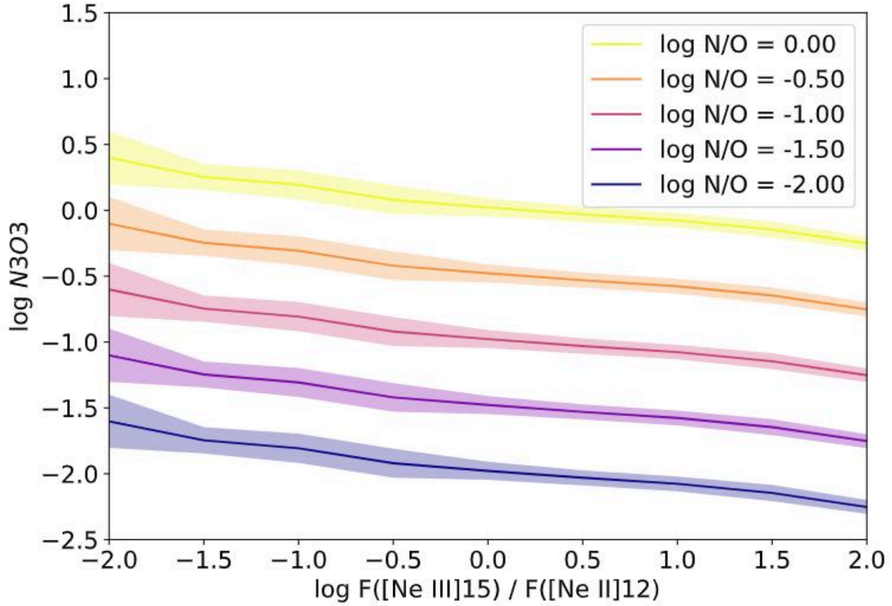

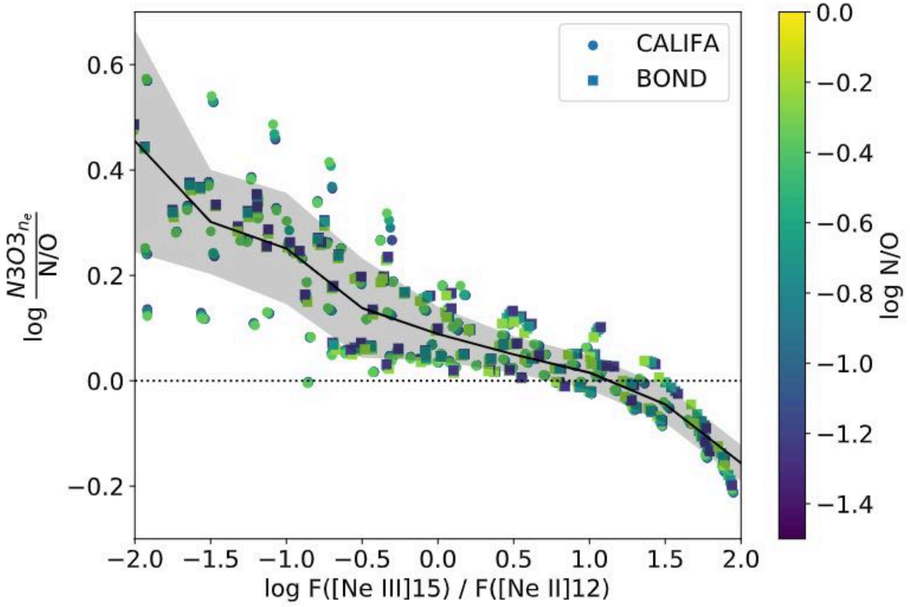

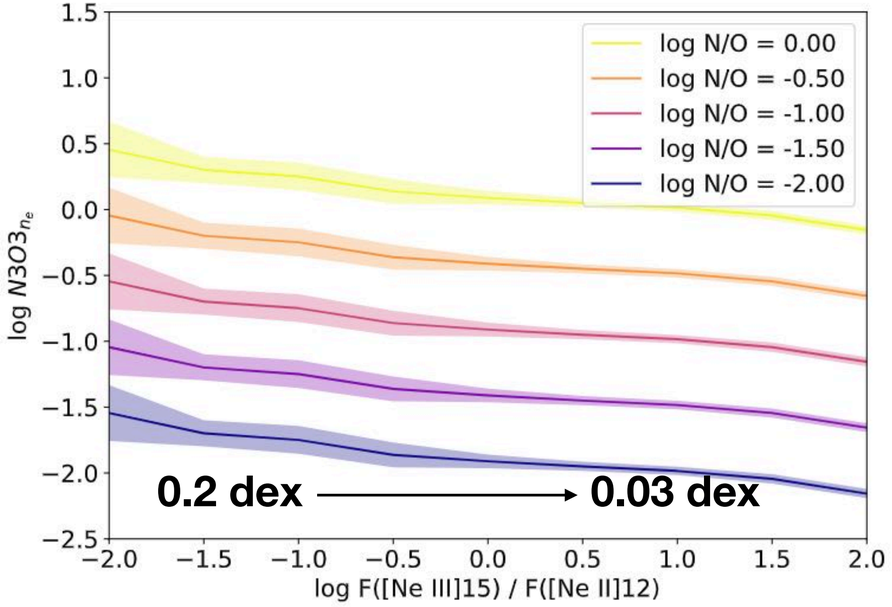

9 regions in 8 local galaxies

- **4 LIRGs**
- **1 SF galaxy nucleus**
- **3 dwarf galaxies**

Galaxy name	Type	Redshift
Arp 299	Interacting LIRG	0.010300
Haro 3	BCD	0.003149
II Zw 40	BCD	0.002632
M 83	Spiral	0.001711
MCG+12-02-001	LIRG	0.015698
NGC 2146	LIRG	0.002979
NGC 4194	LIRG	0.008342
NGC 4214	BCD	0.000970

For NGC 4214 only region I is used

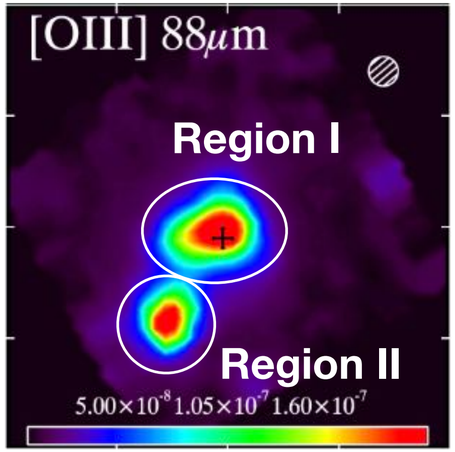

Herschel/PACS (Cormier et al. 2015)

2 components:

Arp 299A and

Arp 299B&C

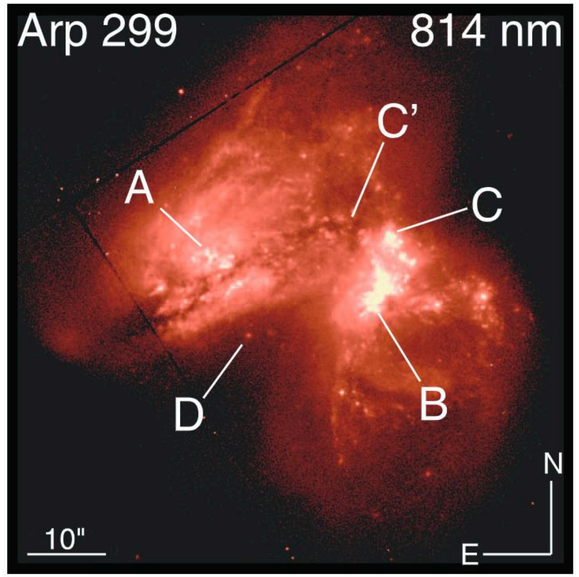

HST/WFPC2 (Neff et al. 2004)

limited by data available

Need for SOFIA

- [O III]52 outside of Herschel/PACS
- [N III] very dim
- Sparse simultaneous detection for [N III] and [O III]52

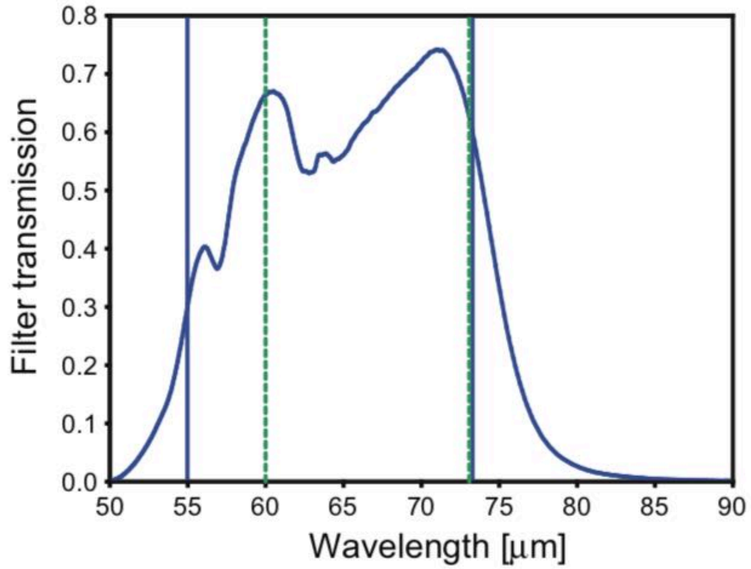

(Poglitsch et al. 2010)

SOFIA/FIFI-LS

- **IFU similar to PACS**
- **50 - 100 μm (blue)**

Application: SOFIA/FIFI-LS [O III]52

Arp 299 A [O III]52

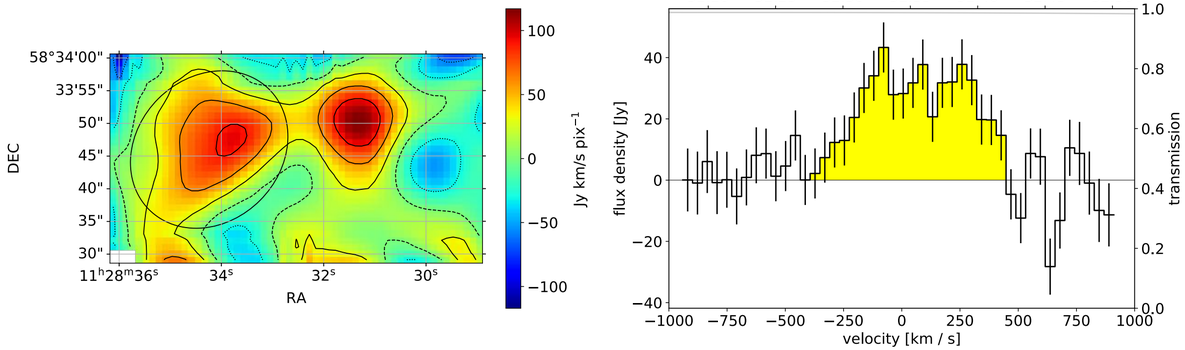

Arp 299 B&C [O III]52

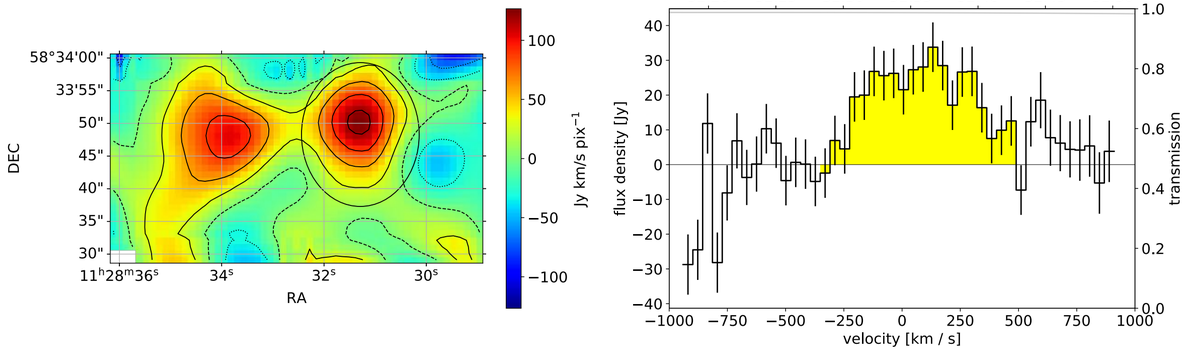

Haro 3 [O III]52

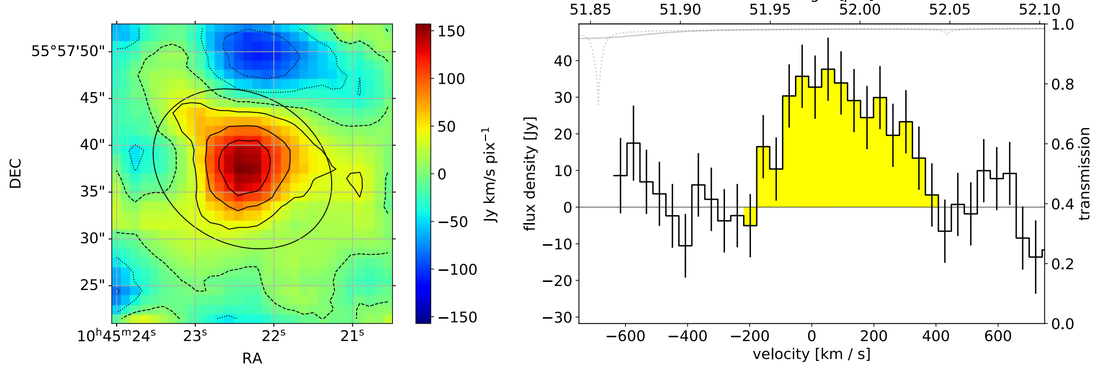

II Zw 40 [O III]52

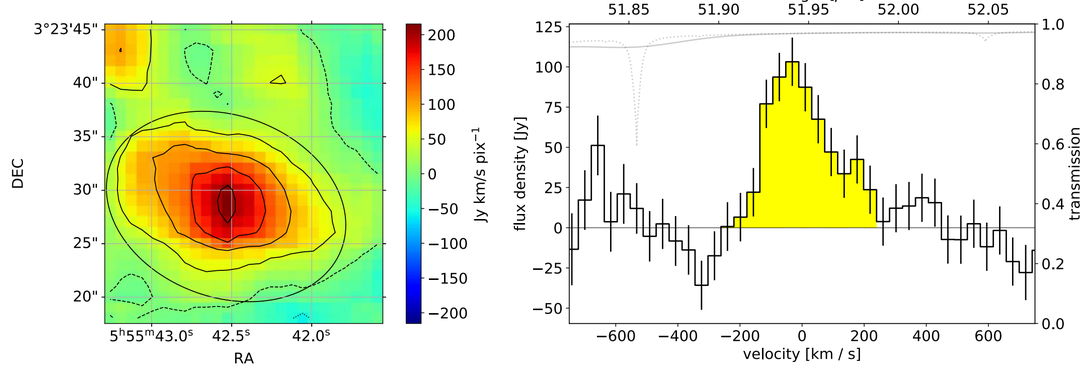

M 83 nuclei [O III]52

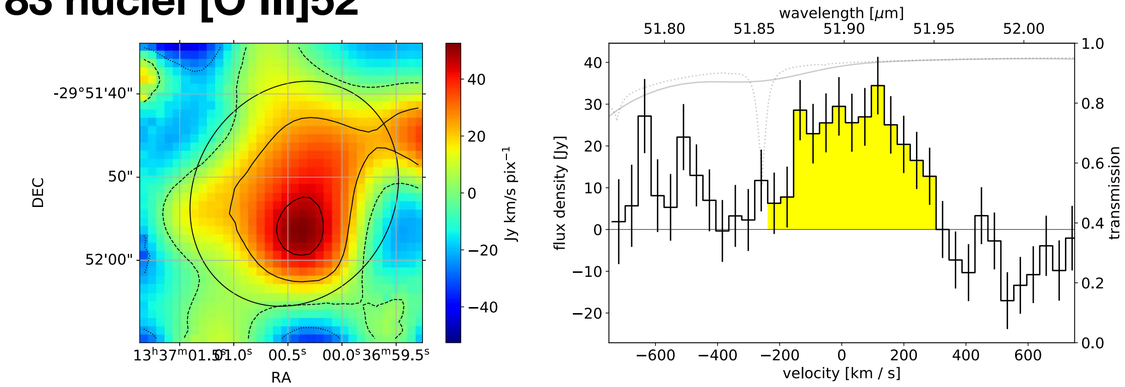

MCG+12-02-001 [O III]52

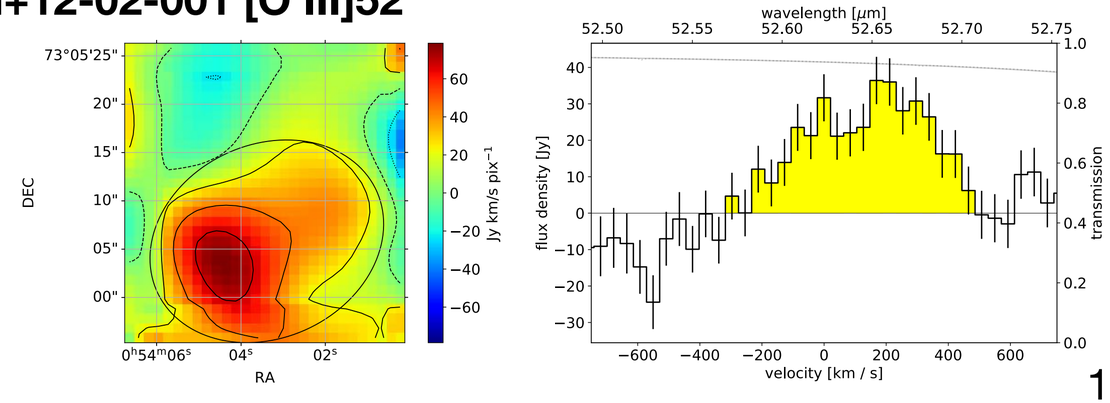

Application: SOFIA/FIFI-LS [O III]52 and [N III]

NGC 4194 [O III]52

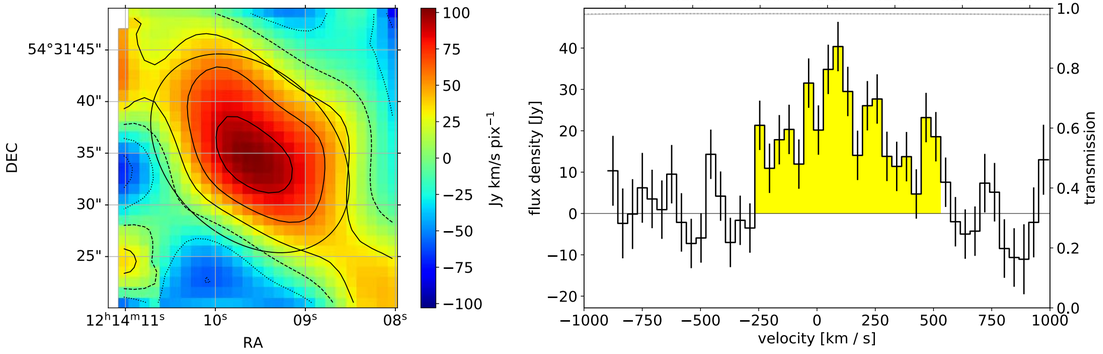

NGC 4214 region I [O III]52

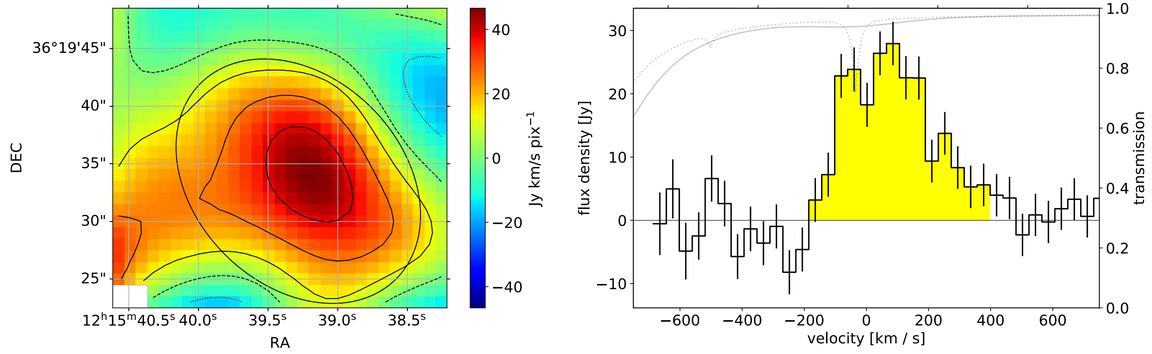

II Zw 40 [N III]

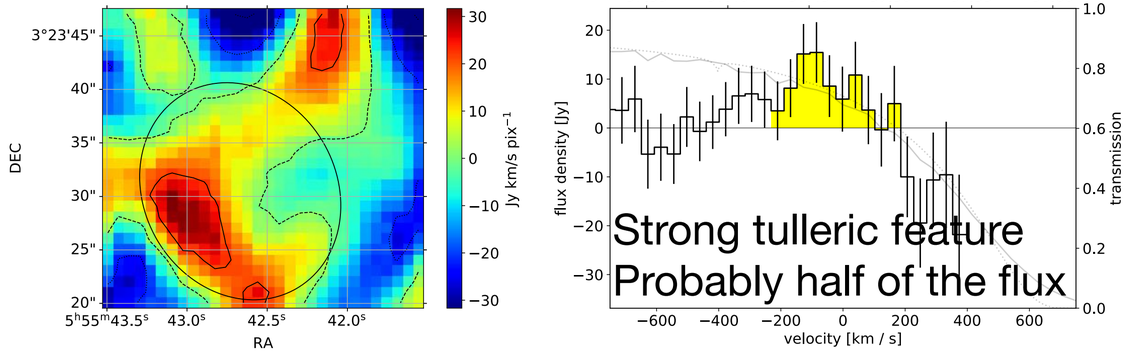

MCG+12-02-001 [N III]

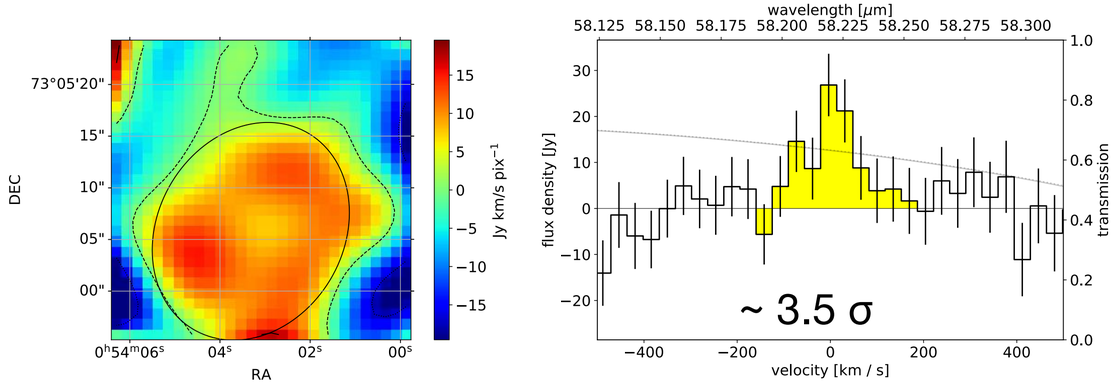

NGC 4214 region I [N III]

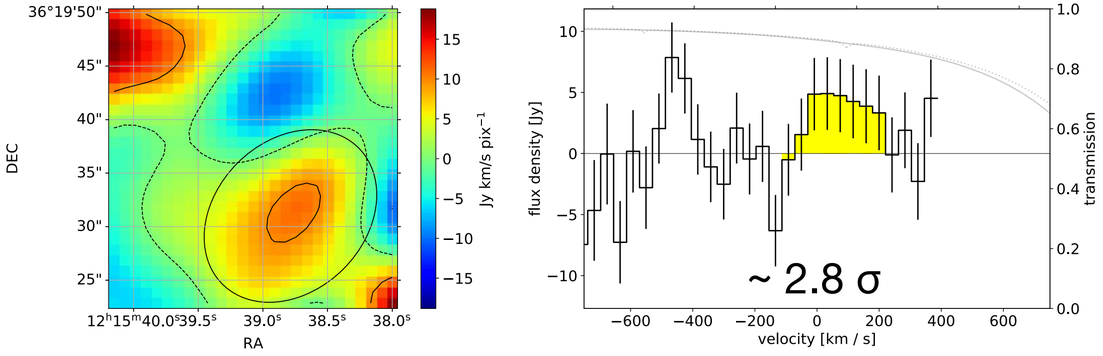

Application: ancillary data

Galaxy name	[N III]	[O III]52	[O III]88	[Ne II]12	[Ne III]15
Arp 299 A	7.3 ± 0.5[a]	40.0 ± 4.28	28 ± 0.32[a]	23.7 ± 0.26[b]	5.70 ± 0.098[b]
Arp 299 B&C	7.2 ± 0.13[a]	30.8 ± 3.72	30 ± 0.26[a]	10.4 ± 0.27[b]	5.44 ± 0.098[b]
Haro 3	1.23 ± 0.17[c]	26.9 ± 2.99	18.4 ± 0.4[c]	3.52 ± 0.13[c]	9.84 ± 0.74[c]
II-Zw 40	5.51 ± 4	48.6 ± 4.52	35.9 ± 0.4[c]	0.735 ± 0.079[c]	14.1 ± 0.9[c]
M83 nucleus	16.6 ± 1.03[d]	22.7 ± 3.03	21.7 ± 0.70[d]	50.3 ± 1.98[d]	2.93 ± 0.077[d]
MCG+12-02-001	5.29 ± 1.53	30.5 ± 3.09	23.4 ± 2.4[e]	20.1 ± 0.21[b]	3.7 ± 0.067[b]
NGC 2146	55.1 ± 5.9[e]	151.4 ± 20.1[e]	157.7 ± 6.5[e]	68.2 ± 0.80[b]	9.81 ± 0.123[b]
NGC 4194	6.5 ± 2.2[e]	31.5 ± 2.8	20.6 ± 1.4[e]	17.57 ± 0.14[b]	5.62 ± 0.06[b]
NGC 4214 region I	1.96 ± 0.70	17.5 ± 1.31	31.9 ± 0.62[f]	8.98 ± 0.22[f]	18.7 ± 0.14[f]

SOFIA/FIFI-LS

ISO

Herschel/PACS: all the rest of far-IR data

Spitzer/IRS: all mid-IR data

Electron density cluster around 200 to 400 cm^-3 except NGC 4214

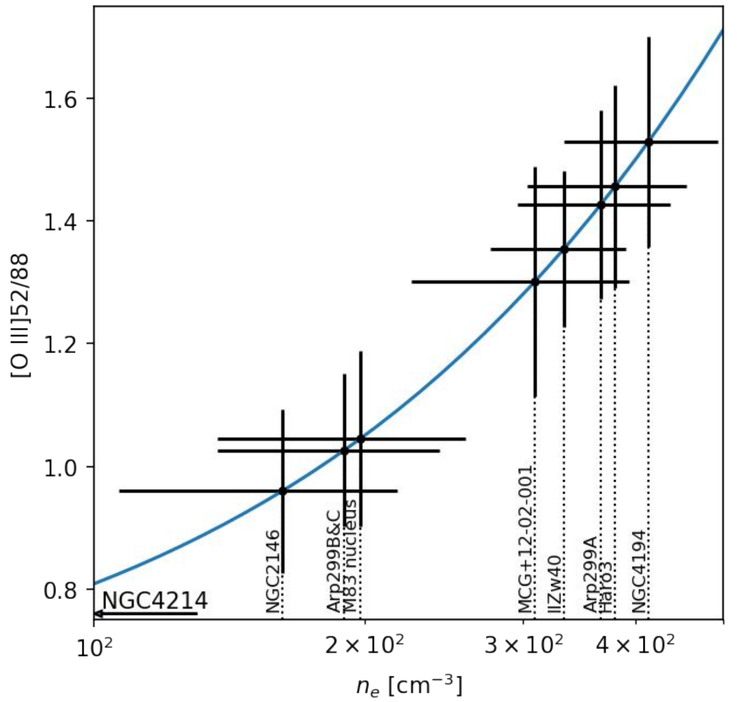

Application: results

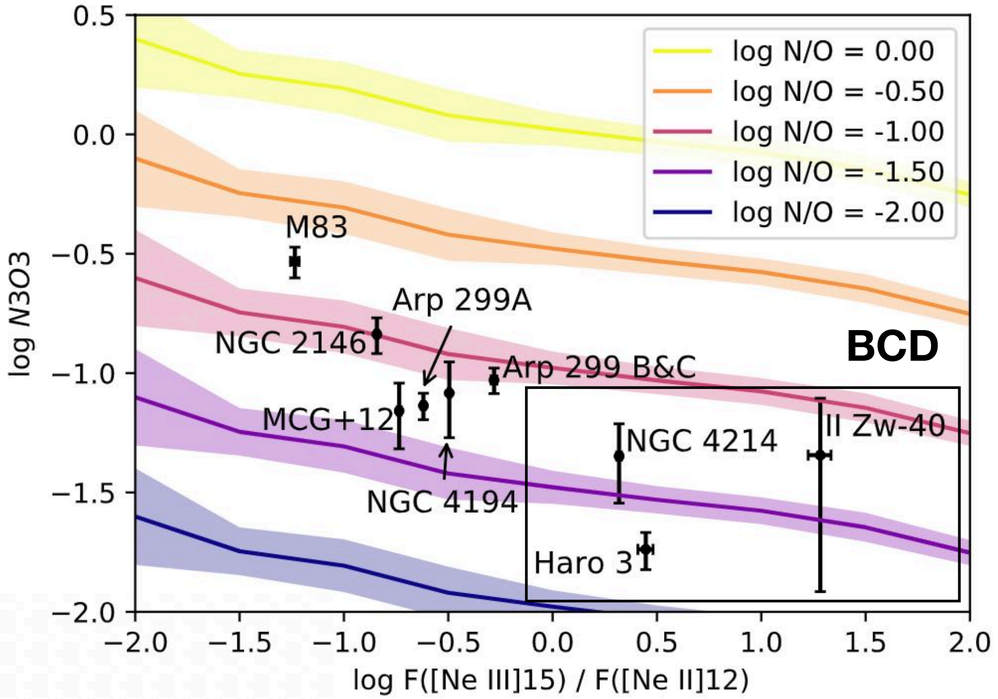

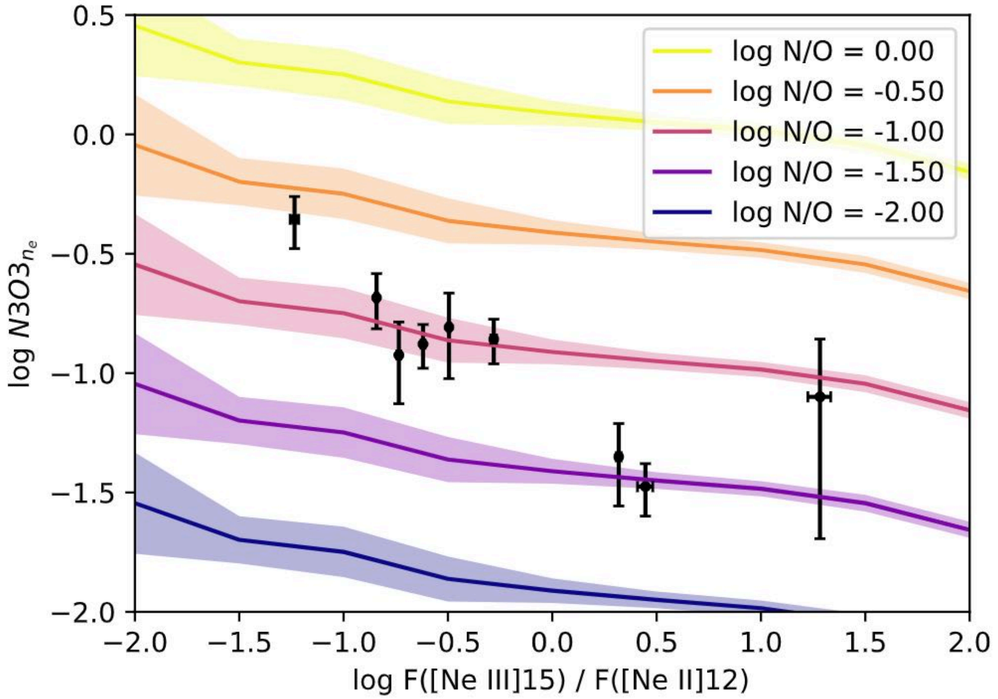

Galaxy Name	Strong Line Method		Model Calibration		log [Ne III]/[Ne II]
	log $N3O3$	log $N3O3_{ne}$	log N/O by N3O3	log N/O by N3O3$_{ne}$	
(1)	(2)	(3)	(4)	(5)	(6)
Arp 299 A	$-1.14^{+0.052}_{-0.059}$	$-0.88^{+0.082}_{-0.101}$	$-1.24^{+0.119}_{-0.164}$	$-1.04^{+0.122}_{-0.171}$	−0.62
Arp 299 B&C	$-1.03^{+0.050}_{-0.057}$	$-0.86^{+0.083}_{-0.103}$	$-1.08^{+0.102}_{-0.133}$	$-0.97^{+0.109}_{-0.145}$	−0.28
Haro 3	$-1.74^{+0.071}_{-0.085}$	$-1.48^{+0.096}_{-0.124}$	$-1.71^{+0.089}_{-0.113}$	$-1.53^{+0.101}_{-0.133}$	0.45
II Zw 40	$-1.34^{+0.239}_{-0.572}$	$-1.10^{+0.242}_{-0.594}$	$-1.23^{+0.242}_{-0.595}$	$-1.08^{+0.243}_{-0.602}$	1.28
M83 nucleus	$-0.53^{+0.060}_{-0.069}$	$-0.36^{+0.096}_{-0.123}$	$-0.75^{+0.118}_{-0.163}$	$-0.63^{+0.134}_{-0.195}$	−1.23
MCG+12-02-001	$-1.16^{+0.116}_{-0.159}$	$-0.92^{+0.138}_{-0.204}$	$-1.29^{+0.152}_{-0.237}$	$-1.12^{+0.163}_{-0.264}$	−0.73
NGC 2146	$-0.84^{+0.068}_{-0.081}$	$-0.68^{+0.100}_{-0.131}$	$-0.99^{+0.126}_{-0.177}$	$-0.90^{+0.137}_{-0.201}$	−0.84
NGC 4194	$-1.08^{+0.130}_{-0.187}$	$-0.81^{+0.143}_{-0.215}$	$-1.16^{+0.162}_{-0.261}$	$-0.95^{+0.164}_{-0.267}$	−0.49
NGC 4214 region I	$-1.35^{+0.135}_{-0.197}$	$-1.35^{+0.139}_{-0.206}$	$-1.34^{+0.145}_{-0.219}$	$-1.41^{+0.143}_{-0.215}$	0.32

In the case of no Neon line

- LIRG: N3O3
- Dwarf: N3O3$_{ne}$

Application: comparison

Galaxy	Optical log N/O	Far-IR log N/O
Arp 299 A	$-0.85^{+0.026}_{-0.028}$[a]	$-1.04^{+0.122}_{-0.171}$
Arp 299 B&C	$-0.71^{+0.026}_{-0.028}$[a]	$-0.97^{+0.109}_{-0.145}$
Haro 3	$-1.13^{+0.031}_{-0.033}$[a], $-1.06^{+0.088}_{-0.107}$[b], -1.29[c], -1.35[d],	$-1.53^{+0.101}_{-0.133}$
II Zw 40	$-1.30^{+0.029}_{-0.031}$[a], -1.44[c], -1.44[d], $-1.052^{+0.059}_{-0.077}$[e]	$-1.08^{+0.243}_{-0.602}$
M83	$-0.63^{+0.028}_{-0.042}$[b]	$-0.63^{+0.134}_{-0.195}$
NGC 2146	$-0.77^{+0.029}_{-0.031}$[a], $-1.06^{+0.049}_{-0.059}$[b]	$-0.90^{+0.137}_{-0.201}$
NGC 4194	$-0.59^{+0.026}_{-0.028}$[a], -0.5[c]	$-0.95^{+0.164}_{-0.267}$
NGC 4214 region I	$-1.30^{+0.029}_{-0.031}$[a], $-1.28^{+0.017}_{-0.018}$[b], -1.30[d,e],	$-1.41^{+0.143}_{-0.215}$

N/O in literature

+

N2S2 calculation

+

N2S2 & PG16 photoionisation grid calibration

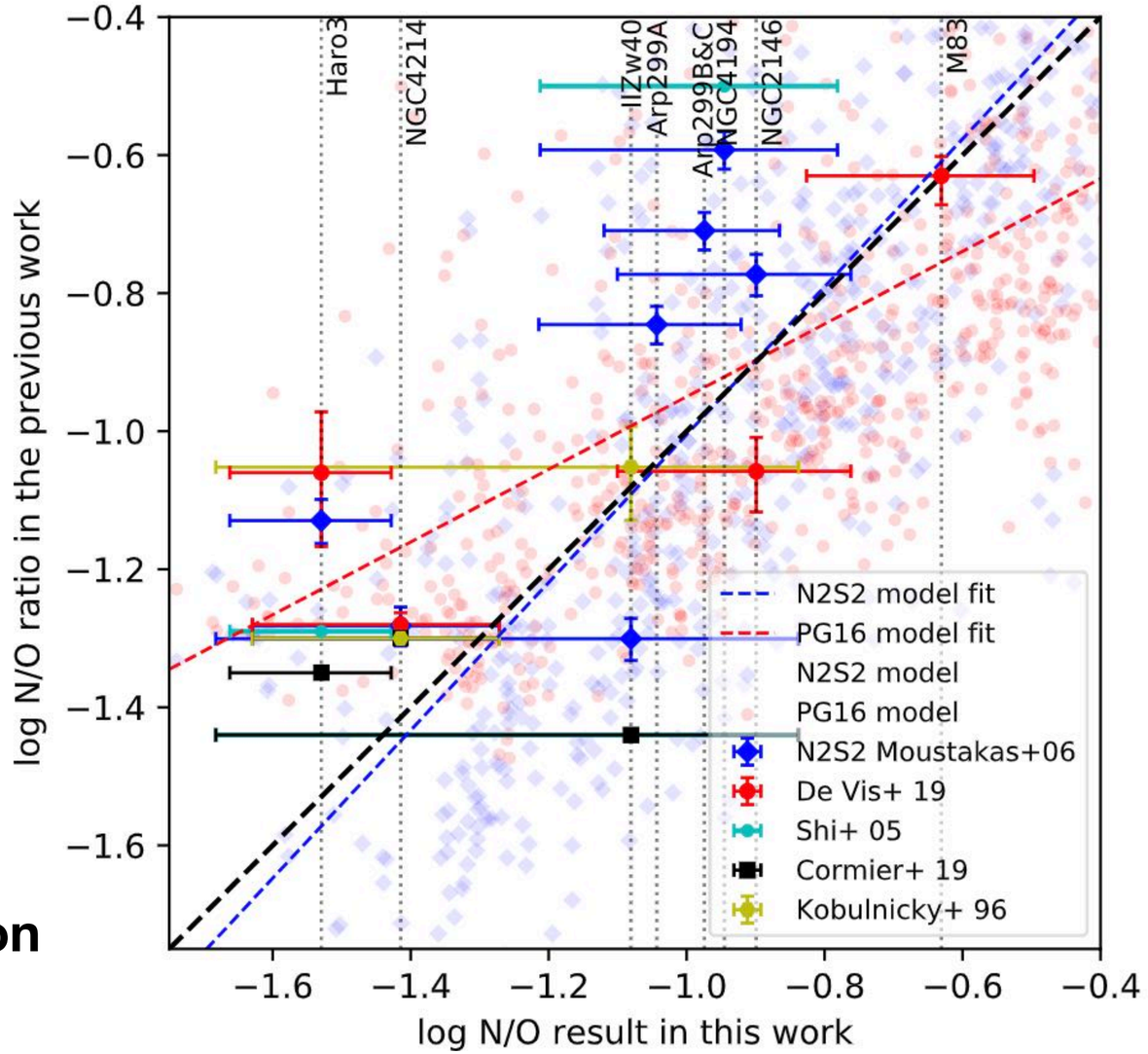

N/O in literature

- De Vis et al. 2019 (4/8 sources, PG16)
- Shi et al. 2005; Cormier et al. 2009; Kobulnicky & Skillman 1996

PG16: -0.657 - 0.201 log N2 + (0.742 - 0.075 log N2) * log(N2/R2)

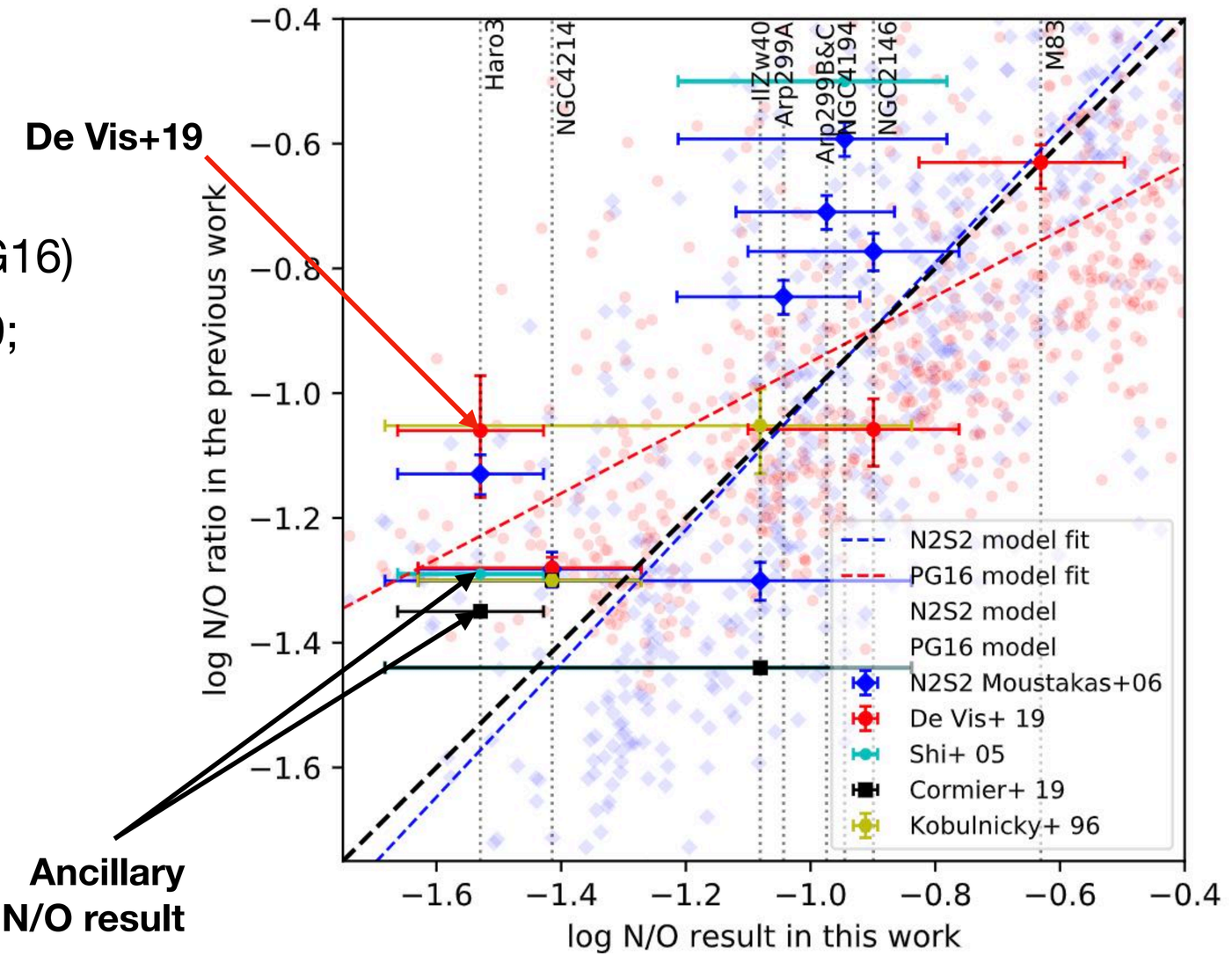

New optical N/O calculation

N2S2: [N II]λ6584/[S II]λ6717+6731

- N2S2 is insensitive to extinction
- Moustakas & Kennicutt (2006) integrated spectroscopy covers the whole galaxy

Model calibration

- N2S2 vs N3O3
- PG16 vs N3O3

N2S2 calculation

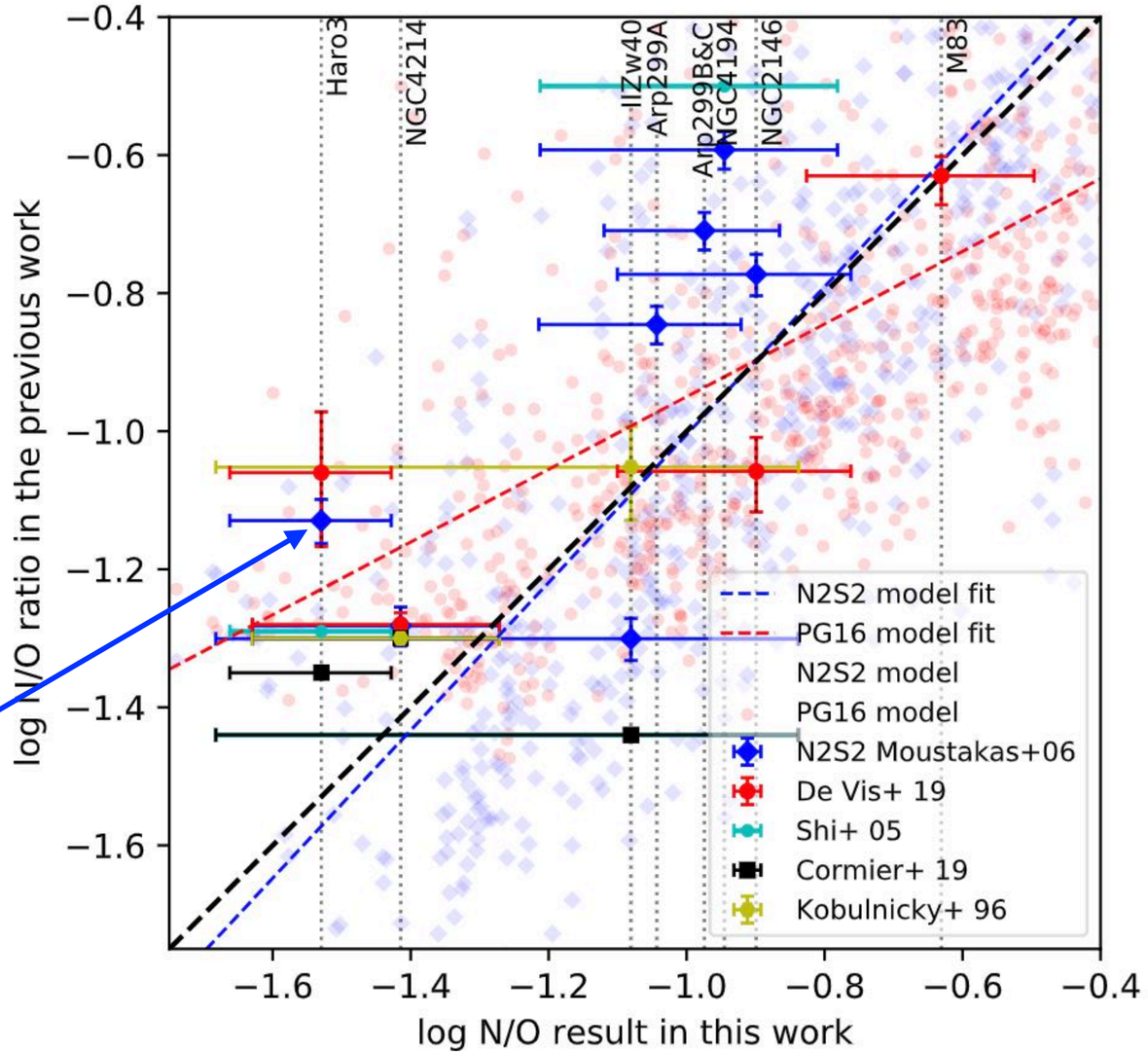

Far-IR to Optical comparison

- FIR and optical N/O follow similar trend
- Large scatter in the reference optical N/O
- N2S2 photoionization grid calibration agrees with N3O3 (blue dashed line); PG16 overestimate at low N/O end, and underestimate at N/O > -0.9
- Large error from FIR data, especially [N III]
- **Optical N/O ~ FIR N/O + 0.2 dex**

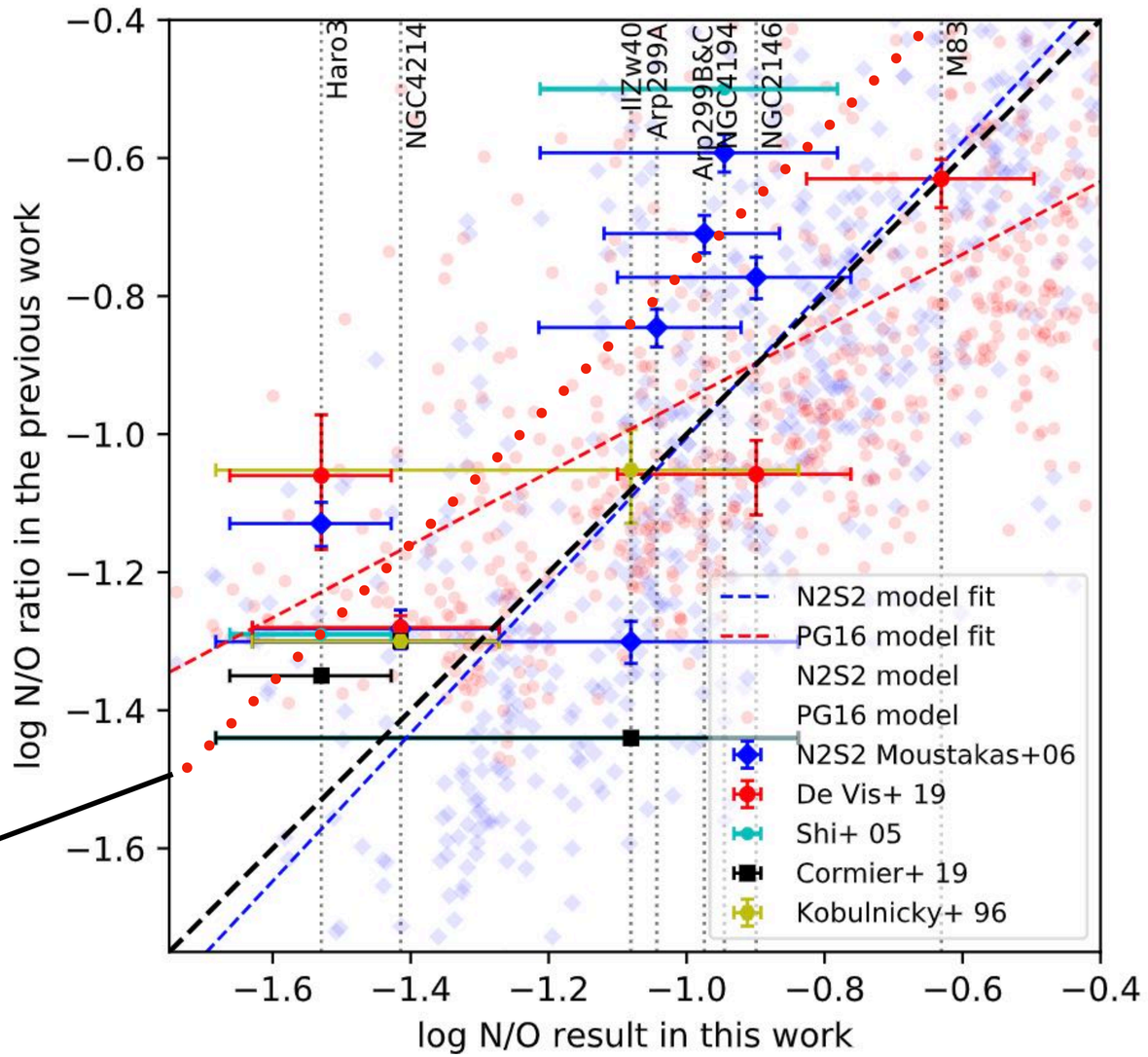

Far-IR to Optical N/O discrepancy

- **Extinction? X**

  Not for N2S2 calculation

- **Optical and Far-IR data mis-match in beam size? X**

  Not for N2S2 calculation

- **ISO beam size larger than SOFIA and Herschel? X**

  Effect <30%, not for NGC 2146, and would overestimate N/O for NGC 4194

- **DIG contamination in optical method?**

  Probably. DIG can contribute to low ionized lines (e.g. [N II]λ6584)

- **Far-IR and optical lines probe H II regions of different physical condition?**

  Probably. Far-IR is density weighted, and highly ionized lines are mainly emitted in hard radiation environment. N3O3 is biased to ISM around massive, dense, young stars.

- [N III]/[O III]52 physically robust probe for N/O
- Density correction
- Radiation hardness calibration with [Ne III]15/[Ne II]12
- Demonstrate on local LIRGs and dwarf galaxies
- FIR - optical trend agrees, see 0.2 dex discrepancy
- Limited by sample size and noisy [N III] observation
- Prospective application:
  - more SOFIA/FIFI-LS data
  - on high redshift galaxies (dwarf like, some with [O III]88)